Origin of α-satellite repeat arrays from mitochondrial molecular fossils - sequential insertion, expansion, and evolution in the nuclear genome

Yihang Zhou[1]

[1]*School of Life Sciences and Technology, Tongji University, Shanghai, China*

Keywords: mitochondrion, satellite sequences, palindromic repeats, NuMT (nuclear mitochondrial DNA), gene conversion

Abstract

Alpha satellite DNA is large tandem arrays of 150-400 bp units, and its origin remains an evolutionary mystery. In this research, we identified 1,545 alpha-satellite-like (SatL) repeat units in the nuclear genome of jewel wasp *Nasonia vitripennis*. Among them, thirty-nine copies of SatL were organized in two palindromic arrays in mitochondria, resulting in a 50% increase in the genome size. Strikingly, genomic neighborhood analyses of 1,516 nuclear SatL repeats revealed that they are located in NuMT (nuclear mitochondrial DNA) regions, and SatL phylogeny matched perfectly with mitochondrial genes and NuMT pseudogenes. These results support that SatL arrays originated from ten independent mitochondria insertion events into the nuclear genome within the last 500,000 years, after divergence from its sister species *N. giraulti*. Dramatic repeat GC-percent elevation (from 33.9% to 50.4%) is a hallmark of rapid SatL sequence evolution in mitochondria due to GC-biased gene conversion facilitated by the palindromic sequence pairing of the two mitochondrial SatL arrays. The nuclear SatL repeat arrays underwent substantial copy number expansion, from 12-15 (SatL1) to over 400 copies (SatL4). The oldest SatL4B array consists of four types of repeat units derived from deletions in the AT-rich region of ancestral repeats, and complex high-order structures have evolved through duplications. We also discovered similar repeat insertions into the nuclear genome of *Muscidifurax*, suggesting this mechanism can be common in insects. This is the first report of the mitochondrial origin of nuclear satellite sequences, and our findings shed new light on the origin and evolution of satellite DNA.

Introduction

Satellite sequences are arrays of repetitive non-coding DNA sequences. Unlike other tandem repeats such as microsatellite (2-5bp unit size in several hundred copies) and minisatellite (~15bp repeats in 0.5-30 Kb arrays), satellite sequences are organized in much larger tandem arrays with longer repeat units (>100bp) [1]. In humans, alpha satellite DNA sequences are huge arrays of 171-bp monomers, organize in higher-order repeat (HOR) structures [2]. Each HOR contains a certain number of 171 monomers with 50-70% sequence identity among them [2, 3]. Sequence similarity between HORs are quite high (>90%) [4], suggesting that they were derived from recent segmental duplications. HOR structures differ across arrays and chromosomes [5], indicating independent evolutionary history. Collectively, these large arrays account for 10% of the human genome.

For most satellite DNA sequence, the functions remain unknown. Their rapid evolution and next-generation sequencing's natural incompatibility are two major barriers. Based on loci, most satellite DNA can be classified to centromeres satellites, pericentromeric satellites and telomeric/sub-telomeric satellites. In epithelial cancers, Ting et al observed an aberrant overexpression of satellite DNA in mouse pericentromeric satellites and human α satellites, which may suggest a global heterochromatin silencing alteration [6, 7]. Telomeric sequences are a known to function in protecting chromosome ends during cellular processes. Few satellites located in euchromatic regions. Halbach et al. discovered that, the euchromatic satellites can derive piRNA in Aedes. The inactivation of these piRNA would result in developmental arrest and maternal transcripts degradation failure during embryonic development [7, 8].

Evolutionary origin and maintenance of satellite DNAThe satellite DNA evolution is rapid, divergent and underwent selection pressure and stochastic events [9-11]. The main evolution

models include the library hypothesis [12], concerted evolution model [13], centromere drive model [14]. The library hypothesis deems the close species inherit a set of ancestral conserved satellite with species-specific divergency [15, 16]. The concerted evolution model believes the existence of satellite DNA is a natural state as the result of nonrepetitive DNA unequal crossovers [17], which is driven by molecules [18-20]. The centromere drive model is trying to explain the centromere paradox, which is coexistence of the conserved cell division procedure and rapidly evolved centromeric components [21]. In bacterial, the evolution of satellite plasmids itself was proved to elongate the acquired accessory genes maintenance [22]. Our knowledge about the evolution origin of satellite DNA is very limited.

Satellite DNA studies in insects were mainly focused on Drosophila. Flynn et al found the Drosophila virilis satellite DNA rapid dynamics could be explained by various unknown forces at cellular and population level, and centromere drive is likely to explain satellite evolution, expansion and region correlated properties [23]. The pericentromeric satellite DNA in Drosophila plays an important role in chromocenter and associating proteins [24]. Drosophila telomeres are made of specialized retrotransposons, sequence-independent epigenetic structures, whose activity can be tuned via piRNA pathways [25-28]. In general insect satellite DNA, the evolutionary conservation features were identified, which include but not limit to region length [29], motif pattern, secondary or tertiary structures [30]. However, these features can be very species-specific, such as the satellite DNA structures [31] and gaining rate [32]. The functions and evolution of satellite DNA in insects are still poorly understood [33]. The library hypothesis was used in explaining genus Schistocerca satellite DNA evolution [15, 34]. The centromere driven model was observed in Drosophila [14, 35] and ants [36]. Different evolution hypothesis

coexist in the same Drosophila species, which indicates another uncovered insect satellite DNA derivation hypothesis.

Results

Discovery and characterization of mitochondrial SatL tandem repeats in the nuclear genome of *Nasonia vitripennis* (*Nv*)

In order to understand the origin of *Nv* mitochondrial SatL tandem repeats, we first sought to identify if there is any distantly related homologs in the Nv genome. We conducted a local BLASTN search against the Nv genome (both nuclear and MT) using a MT-SatL repeat unit as a query. Interestingly, in addition to the MT-SatL repeats, the search returned several short sequence hits of 70 bp long that display a match with a part of the MT-SatL sequence (sequence identity around 70% and e-value around 7e-06). When looking more into the hits, we realized that many of these hit seqeunces are arranged adjacently in certain genomic loci, a phenomenon similar to SatL repeats on mitochondria. We extracted the corresponding genomic regions and conducted both pair-wise BLASTN searches and tandem repeat finder (TRF) analysis. Both of them revealed the presence of many novel tandem repeats in these genomic regions. To further confirm the relationship, we conducted reciprocal BLASTN searches with several of these new repeats which indeed identified the MT-SatL repeats as the best hits. In order to comprehensively identify all the repeat loci, we conducted a series of new BLASTN searches using the repeat units of previous analysis, which led a collection of about 1,500 novel repeat sequneces from about 20 genomic loci in the Nv nuclear genome (Table S1). A multiple sequence alignment of all collected repeat sequences (Figure 1A and Data S1) further revealed that despite the repeat sequences have varible size (from 137bp to 257bp) and relatively low sequence identity, they do display a strong conservation across the repeat sequence. Especially, two regions appear to be the conservation cores, second of which is the region revealing the similarity in the the most of the above BLASTN searches.

To further understand their relationship, we conducted a phylogenetic analysis using the FastTree method under the model. We found the repeat sequences from each genomic locus are clustered together and many of them can be further grouped into higher order. Thus, according to their tree distance and sequence similarity between clusters, we divided them into four major classes (Table S1 and Figure 1C). Among them, three classes, SatL2-4, contain only the repeats from nuclear genomes whereas the Sat1 class contain the original MT-SatL repeats (named SatL1A) and two other nuclear repeat regions.

SatL repeats are absent in closely related wasp species and cause a *Nv*-specific enrichment of satellite sequences

We also tried to identify repeat homologs in other wasp genomes (including Ng, No, Ni, Ts) using above-mentioned search strategies. However, no significant hits can be found. To further examine the difference between these genomes, we utilize the repeat masker.

Genomic neighborhood analysis reveals an association between nuclear SatL repeats and NuMT elements

We next conducted a comprehensive genome neighborhood analysis to understand the genomic context of the newly-identifed repeats. We found that among 10 examined nuclear genomic loci, nice loci contain nuclear-mitochondrial (NuMT) genes or armR element (Figure 2A). Many of these NuMT genes are inactive by containing the deletion or insertion. Additionally, we also identified many transposible elements, including LTR retrotransposon, LINE elements and several DNA transposons, in these genomic loci. Many of them have inserted into the NuMT genes which inactivated them. NuMT has been well studied and they are known to originate from several independent transfers from mitochondria to nuclear genome. In the mitochondrial

genome, the SatL1A repeats are located downstream of the *cob* gene and upstream *rrnS* gene. For the newly identified genomic loci, despite many of them missing some of NuMT genes, such locational order is still retained. This strong genomic association between the SatL repeats and NuMT elements suggests they move as one unit; in other words, the nuclear SatL repeats might have moved to the nuclear genome together with NuMT transfers.

Phylogenetic congruency suggests sequential independent NuMT insertions togehter withnuclear SatL repeats

To test the above hypothesis, we examined congruence between the phylogenetic trees of the repeat units from different classes and their respective associated MT/NuMT genes, including *nad2*, *nad6* and *cob* (Figure 2B). The assumption is that if they move as one unit during evolution, the evolutionary histories between them should be indential. We used three phylogenetic methods (Maximum Likelihood, Bayesian inference and FastTree) to infer the relationship between repeats; all of them produced a same tree topology (Figure 2B), consistent with the phylogeny based all repeat sequences reported earlier (Figure 1C). For MT/NuMT genes, we generate a concatenated sequence containing *nad2*, *nad6* and *cob*, and computed their maximum likelihood tree using their 3rd codon positions. These analyses revealed a highly similar topological congruence between SatL repeats and associated MT/NuMt genes. This strongly supports the comobility of SatL repeats with the asscoatied NuMT genes during the course of transfers from mitochondria to nucleus. It is conceivable that mitochondria genome which contain carry both repeats and other typical MT genes has undergone a series of sequential transfers to nucleus during evolution. As NuMT genes are non-functional in nuclear genome, many of them have been lost or inactiviated due to the gene mutation/deletion or intertion by

transposable elements. While for repeat region, they have been greatly expanded due to their unique hairpin sturucture which can faciliates the replication slippage.

Discussion

This study uncovers a striking case of satellite DNA in Nasonia vitripennis that originates from mitochondrial sequences (SatL) rather than the nuclear genome, offering new insights into the evolutionary plasticity of satellite repeats. Multiple independent transfer events from mitochondria to the nucleus generated tandem arrays of SatL repeats adjacent to NuMT pseudogenes, with phylogenetic analyses confirming their shared evolutionary history. These repeated insertions likely occurred within the last 500,000 years, underscoring the rapid tempo of SatL evolution. In mitochondria, SatL repeats exhibit marked GC enrichment, presumably driven by GC-biased gene conversion facilitated by palindromic structures. Once integrated into the nucleus, they underwent substantial copy number expansion, creating diverse repeat classes (SatL1–4) that vary in size and sequence identity.

Notably, the formation of higher-order repeat structures and partial sequence deletions suggests frequent duplication events and rearrangements in older arrays, revealing the dynamic nature of satellite DNA evolution. The absence of similar repeats in closely related wasp species implies that SatL amplification is a lineage-specific phenomenon. Moreover, preliminary evidence in Muscidifurax indicates that mitochondrial sequence insertions may be more widespread in insects than previously thought. Taken together, these results highlight an unconventional origin of nuclear satellite DNA and its intricate interplay with genome architecture.

Materials and Methods

Wasp nuclear and mitochondrial genome assemblies.

The mitochondrial genome assembly and annotations were published in our previous research [37].

SatL repeats identification, characterization, alignment, and phylogenetic analysis in the Nv mitochondrial and nuclear genome.

In order to identify the distant homologs of SatL repeats, we performed the local BLASTN searches using a SatLA1 repeat unit as a query (PMID: 9254694) against nuclear and mitochondrial genomes of Nasonia vitripennis AsymCx strain with a search word size of 11 and a cut-off e-value of 0.05. For the short sequence hits, we utilize a reciprocal BLASTN search strategy to confirm their relationship with the query.

To locate the repeat region and isolcate the requence sequence, the large genomic region was extracted and subjected to both pair-wire BLASTN comparisons and Tandem Repeat Finder (TRF) prediction (PMID: 9862982). Manual retrieval and adjustment were also conducted to correct the bourdrey of the repeat when automatic methods failed to collect the sequences. Multiple sequence alignments were built using the KALIGN (PMID: 16343337) and MUSCLE (PMID: 15034147) programs, followed by careful manual adjustments.

The conservation pattern of the multiple sequence alignment was calculated using a consensus mehod (written in a custom Perl script). Consensus is calculated by the examination of each column of an alignment to determine whether an above-threshold fraction of the residues belongs to a type of nucleotide, where ‘A’ stands for adenine, ‘T’ for thymine, ‘G’ for guanine and ‘C’ for cytosine. The alignments were visualized using CHROMA program (11590103) and further

modified using Adobe Illustrator and Microsoft word. Only matching nucleotides are the highlighted using black background and white font color, and their consensus is labeled below alignments.

Phylogenetic analysis of the SatL repeats was conducted using the FastTree method with GTR model.

Genomic neighborhood annotation of *Nv* nuclear SatL repeats

To annotate the ORFs recovered from the repeat-containing loci, we used BLASTN, BLASTX to identify the homologs in NCBI non-redendunt database. We also used repeat masker to identify the potential transposable elements. For nucleotide sequences, pair-wise BLASTN comparison was used to identify the repetitive regions. For potential protein-coding genes and pseudogenes, we generated the MSA of their protein homologs and defined domains to correct the annotation errors.

Phylogenetic analysis of mitochondrial genes and NuMT pseudogenes.

To construct the phylogenetic tree of repeat units from different classes, we utlized three methods, including Maximum Likelihood (ML) analysis implemented in the MEGA7 program (27004904), an approximately-maximum-likelihood method implemented in the FastTree 2.1 program (19377059), and Bayesian Inference implemented in the BEAST 2.6.3 program (30958812). For ML analysis, the evolutionary history was inferred based on the General Time Reversible (GTR) model. Initial tree(s) for the heuristic search were obtained automatically by applying Neighbor-Join and BioNJ algorithms to a matrix of pairwise distances estimated using the Maximum Composite Likelihood (MCL) approach, and then selecting the topology with superior log likelihood value. A discrete Gamma distribution was used to model evolutionary

rate differences among sites (4 categories). The rate variation model allowed for some sites to be evolutionarily invariable. Codon positions included were only 3rd, for cob-nad6-nad2 concatenated gene tree, while the rest used all positions. A bootstrap analysis with 100 repetitions was performed to assess the significance of phylogenetic grouping. For FastTree analysis, the GTR evolutionary models with default parameters were applied, which include the discrete gamma model with 20 rate categories. For Bayesian inference, the Hasegawa-Kishino-Yano model (HKY) model with a discrete Gamma distribution (four rate categories) was used to model evolutionary rate differences among sites. Markov chain Monte Carlo (MCMC) duplicate runs of 10 million states each, sampling every 1,000 steps was computed. Logs of MCMC runs were examined using Tracer 1.7.1 program. Burn-ins were set to be 2% of iterations.

To infer the evolutionary history of MT/NuMT genes, we generated a concatenated sequence containing *nad2*, *nad6* and *cob* which are contained by most of the repeat loci, and computed their maximum likelihood tree using their 3rd codon positions with the GTR model.

Both trees with the highest log likelihood from the ML analysis were visualized using the MEGA7 program. The bootstrapping values from ML analysis, the SH-like local support values from FastTree analysis and the Posterior values from Bayesian inference analysis are shown next to the branches.

References

1. Charlesworth, B., P. Sniegowski, and W. Stephan, *The evolutionary dynamics of repetitive DNA in eukaryotes.* Nature, 1994. **371**(6494): p. 215-20.
2. Willard, H.F., *Chromosome-specific organization of human alpha satellite DNA.* Am J Hum Genet, 1985. **37**(3): p. 524-32.
3. Manuelidis, L., *Chromosomal localization of complex and simple repeated human DNAs.* Chromosoma, 1978. **66**(1): p. 23-32.
4. Koga, A., et al., *Evolutionary origin of higher-order repeat structure in alpha-satellite DNA of primate centromeres.* DNA Res, 2014. **21**(4): p. 407-15.
5. Sullivan, L.L., K. Chew, and B.A. Sullivan, *alpha satellite DNA variation and function of the human centromere.* Nucleus, 2017. **8**(4): p. 331-339.
6. Ting, D.T., et al., *Aberrant Overexpression of Satellite Repeats in Pancreatic and Other Epithelial Cancers.* Science, 2011. **331**(6017): p. 593-596.
7. *Polish biotechnology on the rise in pandemic.* Przemysl Chemiczny, 2020. **99**(10): p. 1429-1429.
8. Halbach, R., et al., *A satellite repeat-derived piRNA controls embryonic development of Aedes.* Nature, 2020. **580**(7802): p. 274-+.
9. Melters, D.P., et al., *Comparative analysis of tandem repeats from hundreds of species reveals unique insights into centromere evolution.* Genome Biology, 2013. **14**(1).
10. Lower, S.S., et al., *Satellite DNA evolution: old ideas, new approaches.* Current Opinion in Genetics & Development, 2018. **49**: p. 70-78.
11. Plohl, M., N. Mestrovic, and B. Mravinac, *Satellite DNA Evolution.* Repetitive DNA, 2012. **7**: p. 126-152.
12. Mestrovic, N., et al., *Evolution of satellite DNAs from the genus Palorus - Experimental evidence for the "library" hypothesis.* Molecular Biology and Evolution, 1998. **15**(8): p. 1062-1068.
13. Smith, G.P., *Evolution of Repeated DNA Sequences by Unequal Crossover.* Science, 1976. **191**(4227): p. 528-535.
14. Malik, H.S. and S. Henikoff, *Adaptive evolution of Cid, a centromere-specific histone in Drosophila.* Genetics, 2001. **157**(3): p. 1293-8.
15. Palacios-Gimenez, O.M., et al., *Eight Million Years of Satellite DNA Evolution in Grasshoppers of the Genus Schistocerca Illuminate the Ins and Outs of the Library Hypothesis.* Genome Biology and Evolution, 2020. **12**(3): p. 88-102.
16. del Bosque, M.E.Q., et al., *A satellite DNA evolutionary analysis in the North American endemic dioecious plant Rumex hastatulus (Polygonaceae).* Genome, 2011. **54**(4): p. 253-260.
17. Perelson, A.S. and G.I. Bell, *Mathematical models for the evolution of multigene families by unequal crossing over.* Nature, 1977. **265**(5592): p. 304-10.
18. Liao, D., et al., *Concerted evolution of the tandemly repeated genes encoding human U2 snRNA (the RNU2 locus) involves rapid intrachromosomal homogenization and rare interchromosomal gene conversion.* EMBO J, 1997. **16**(3): p. 588-98.
19. Rice, W.R., *A Game of Thrones at Human Centromeres II. A new molecular/evolutionary model.* bioRxiv, 2019: p. 731471.
20. Kobayashi, T. and A.R. Ganley, *Recombination regulation by transcription-induced cohesin dissociation in rDNA repeats.* Science, 2005. **309**(5740): p. 1581-4.
21. Henikoff, S., K. Ahmad, and H.S. Malik, *The centromere paradox: stable inheritance with rapidly evolving DNA.* Science, 2001. **293**(5532): p. 1098-102.
22. Zhang, X., et al., *Evolution of satellite plasmids can prolong the maintenance of newly acquired accessory genes in bacteria.* Nature Communications, 2019. **10**.

23. Flynn, J.M., et al., *Evolutionary Dynamics of Abundant 7-bp Satellites in the Genome of Drosophila virilis.* Molecular Biology and Evolution, 2020. **37**(5): p. 1362-1375.
24. Jagannathan, M., R. Cummings, and Y.M. Yamashita, *The modular mechanism of chromocenter formation in Drosophila.* Elife, 2019. **8**.
25. Batki, J., et al., *The nascent RNA binding complex SFiNX licenses piRNA-guided heterochromatin formation.* Nature Structural & Molecular Biology, 2019. **26**(8): p. 720-+.
26. Raffa, G.D., et al., *Terminin A protein complex that mediates epigenetic maintenance of Drosophila telomeres.* Nucleus, 2011. **2**(5): p. 383-391.
27. Niehrs, C. and B. Luke, *Regulatory R-loops as facilitators of gene expression and genome stability.* Nature Reviews Molecular Cell Biology, 2020. **21**(3): p. 167-178.
28. Cacchione, S., G. Cenci, and G.D. Raffa, *Silence at the End: How Drosophila Regulates Expression and Transposition of Telomeric Retroelements.* Journal of Molecular Biology, 2020. **432**(15): p. 4305-4321.
29. King, L.M. and M.P. Cummings, *Satellite DNA repeat sequence variation is low in three species of burying beetles in the genus Nicrophorus (Coleoptera: Silphidae).* Molecular Biology and Evolution, 1997. **14**(11): p. 1088-1095.
30. Sun, X.P., et al., *Sequence analysis of a functional Drosophila centromere.* Genome Research, 2003. **13**(2): p. 182-194.
31. Palomeque, T., et al., *Characterization and evolutionary dynamics of a complex family of satellite DNA in the leaf beetle Chrysolina carnifex (Coleoptera, Chrysomelidae).* Chromosome Research, 2005. **13**(8): p. 795-807.
32. Wei, K.H.C., et al., *Variable Rates of Simple Satellite Gains across the Drosophila Phylogeny.* Molecular Biology and Evolution, 2018. **35**(4): p. 925-941.
33. Palomeque, T. and P. Lorite, *Satellite DNA in insects: a review.* Heredity, 2008. **100**(6): p. 564-573.
34. Milani, D., et al., *The satellite DNA AflaSAT-1 in the A and B chromosomes of the grasshopper Abracris flavolineata.* Bmc Genetics, 2017. **18**.
35. Bracewell, R., et al., *Dynamic turnover of centromeres drives karyotype evolution in Drosophila.* Elife, 2019. **8**.
36. Huang, Y.C., et al., *Evolution of long centromeres in fire ants.* BMC Evol Biol, 2016. **16**: p. 189.
37. Lin, Z.J., et al., *Comparative analysis reveals the expansion of mitochondrial DNA control region containing unusually high G-C tandem repeat arrays in Nasonia vitripennis.* Int J Biol Macromol, 2020.

Figure legends

Fig. 1. Sequence alignments and phylogenetic analyses of SatL repeats in the mitochondrial and nuclear genome of the jewel wasp *Nasonia vitripennis.*

(A) Multiple-sequence alignment (MSA) of representative sequences of the SatL repeat classes. The repeat classes are highlighted in different colors, except SatL2C and SatL2B: SatL1A in red, SatL1B in orange, SatL1C in purple, SatL2A in lightgreen, SatL2D in green, SatL2E in yellow green, SatL3 in light pink, SatL4B in blue, SatL4A in sky blue. The repeat copy number is shown in bracket. On the left side of MSA, the representative sequences are indicated by their chromosome location, strand information (F for forward, R for reverse) and the corresponding numbering on the repeat locus. The repeat unit sizes are shown on the right side of the MSA. The numbers within sequences are indicative of the excluded residues from sequences. The consensus in 80% of the MSA is shown below the alignment, where 'A' stands for adenine, 'T' for thymine, 'G' for guanine and 'C' for cytosine. Only matching nucleotides are highlighted in black background, except that the matching nucleotides in SatL2C and SatL2B sequences are highlighted in dark grey background. The conserved sequence cores are highlighted below consensus, followed by their sizes. The generation of consensus and visualization refer to methods and materials.

(B) Repeat sequence composition profiles in the genomes of four jewel wasps species in the *Nasonia* genus and another parasitoid wasps in the *Trichomalopsis* genus (***Nv***: *N. vitripennis*; ***Ng***: *N. giraulti*; ***No***: *N. oneida*; ***Nl***: *N. longicornis*; ***Ts***: *T. sarcophagae*).

(C) Evolutionary relationship of different SatL repeat classes. The unrooted phylogenetic tree was constructed by using the FastTree 2.1 program. The SH-like local support values are shown for the major branches only. Different classes are highlighted according to the coloring theme used in MSA (A) and copy numbers are indicated in the bracket.

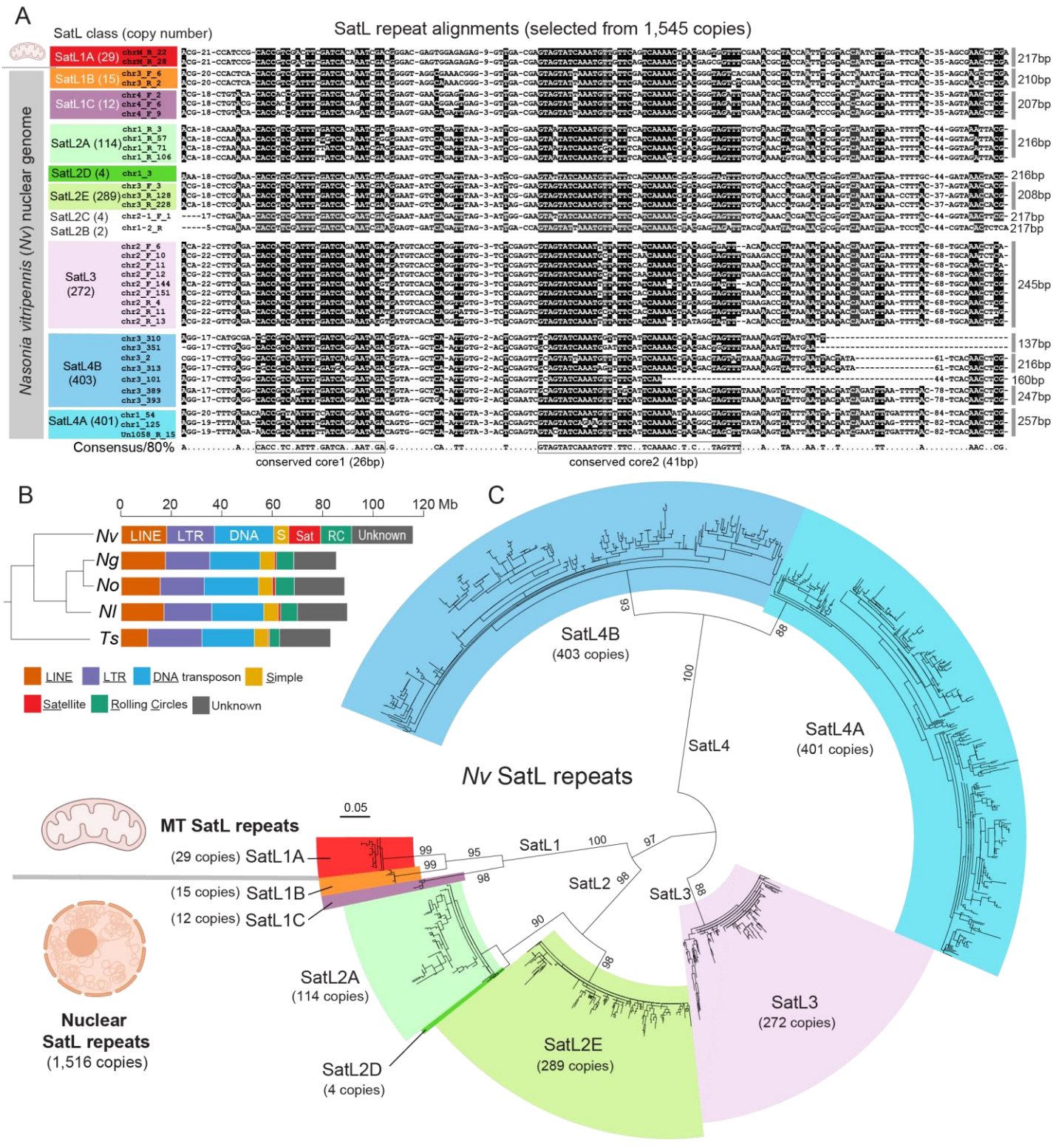
A
SatL class (copy number)
SatL repeat alignments (selected from 1,545 copies)
Nasonia vitripennis (Nv) nuclear genome
SatL1A (29)
SatL1B (15)
SatL1C (12)
SatL2A (114)
SatL2D (4)
SatL2E (289)
SatL2C (4)
SatL2B (2)
SatL3 (272)
SatL4B (403)
SatL4A (401)
217bp
210bp
207bp
216bp
216bp
208bp
217bp
217bp
245bp
137bp
216bp
160bp
247bp
257bp
Consensus/80%
conserved core1 (26bp)
conserved core2 (41bp)
B
0
20
40
60
80
100
120 Mb
Nv
Ng
No
Nl
Ts
LINE
LTR
DNA
S
Sat
RC
Unknown
LINE
LTR
DNA transposon
Simple
Satellite
Rolling Circles
Unknown
C
SatL4B
(403 copies)
SatL4A
(401 copies)
SatL4
Nv SatL repeats
0.05
MT SatL repeats
(29 copies) SatL1A
(15 copies) SatL1B
(12 copies) SatL1C
SatL1
SatL2
SatL3
SatL2A
(114 copies)
SatL2E
(289 copies)
SatL3
(272 copies)
SatL2D
(4 copies)
Nuclear
SatL repeats
(1,516 copies)

Fig. 2. Genomic neighborhood annotations and phylogenetic analyses of SatL repeats and mitochondrial or NuMT (nuclear mitochondrial DNA) genic regions.

(A) Genomic synteny of SatL repeat-containing loci. The repeats, genes and other elements are shown in different shaped boxes with their annotations in or nearby the boxes. For the repeat region, reverse and forward SatL repeats are shown in blue and sky blue triangles, with their copy numbers shown above. Major associated MT genes and transposable elements are highlighted according to the legend at the right-top corner. For SatL4B locus, their repeats can be divided into four subtypes, according to varible repeat unit sizes; therefore they are colored in sky blue, green, yellow and blue, respectively.
(B) Evolutionary association of the SatL repeats (left) with the MT/NuMT genes (right). The phylogeny of SatL repeats from all classes was supported by three methods (ML, BI and FastTree) and the ML tree with the highest log likelihood (-1728.08) is presented with branch supporting bootstrap values in ML, Posterior values in BI and SH-like local support values in FastTree. The phylogeny of three MT/NuMT genes (nad2, nad6 and cob) was inferred using the 3^{rd} codon positions of a concatenated alignment by the ML method with GTR model. The ML tree with the highest log likelihood (-4573.59) is presented with the supporting values from 100 bootstraps. Both trees display a high topological congruence.

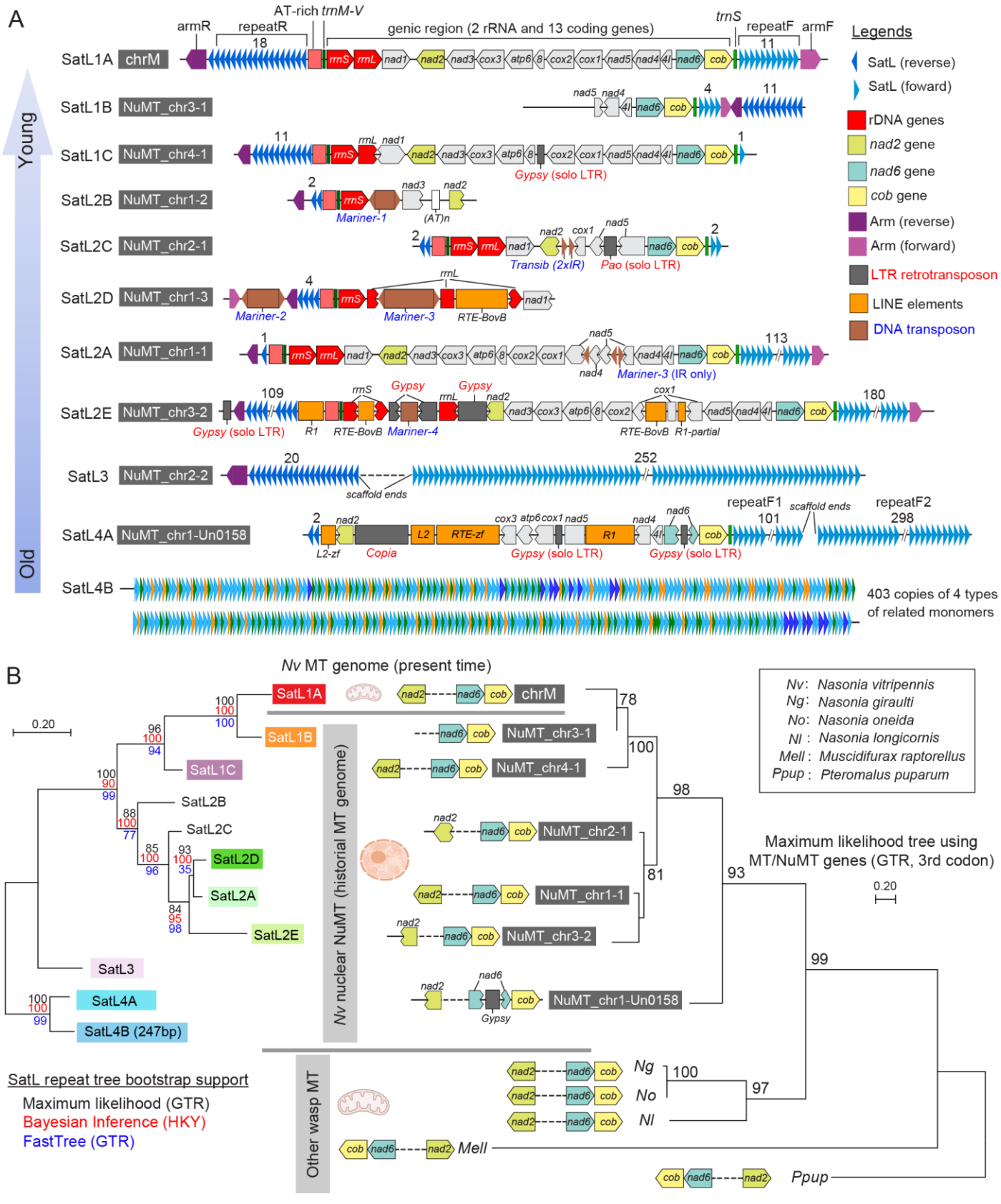
A
Young
Old
armR
repeatR
AT-rich trnM-V
genic region (2 rRNA and 13 coding genes)
trnS
repeatF
armF
Legends
SatL (reverse)
SatL (foward)
rDNA genes
nad2 gene
nad6 gene
cob gene
Arm (reverse)
Arm (forward)
LTR retrotransposon
LINE elements
DNA transposon
SatL1A chrM
SatL1B NuMT_chr3-1
SatL1C NuMT_chr4-1
SatL2B NuMT_chr1-2
SatL2C NuMT_chr2-1
SatL2D NuMT_chr1-3
SatL2A NuMT_chr1-1
SatL2E NuMT_chr3-2
SatL3 NuMT_chr2-2
SatL4A NuMT_chr1-Un0158
SatL4B
Gypsy (solo LTR)
Mariner-1
Transib (2xIR)
Pao (solo LTR)
Mariner-2
Mariner-3
RTE-BovB
Mariner-3 (IR only)
Mariner-4
R1
RTE-BovB
R1-partial
scaffold ends
L2-zf
Copia
L2
RTE-zf
R1
repeatF1
repeatF2
403 copies of 4 types
of related monomers
B
Nv MT genome (present time)
Nv nuclear NuMT (historial MT genome)
Other wasp MT
Nv: Nasonia vitripennis
Ng: Nasonia giraulti
No: Nasonia oneida
Nl : Nasonia longicornis
Mell : Muscidifurax raptorellus
Ppup : Pteromalus puparum
Maximum likelihood tree using
MT/NuMT genes (GTR, 3rd codon)
0.20
SatL repeat tree bootstrap support
Maximum likelihood (GTR)
Bayesian Inference (HKY)
FastTree (GTR)
SatL1A
SatL1B
SatL1C
SatL2B
SatL2C
SatL2D
SatL2A
SatL2E
SatL3
SatL4A
SatL4B (247bp)
NuMT_chr3-1
NuMT_chr4-1
NuMT_chr2-1
NuMT_chr1-1
NuMT_chr3-2
NuMT_chr1-Un0158
Ng
No
Nl
Mell
Ppup

Fig. 3. SatL repeats evolution in the mitochondrial genome and after their insertions into the nuclear genome.

(A) A model of the evolutionary history of SatL repeats. Shortly after the divergence from *Ng* ~1 million years ago, *Nv* acquired the SatL repeats in the mitochondria (MT) genome. At ~500 thousand years ago, there were a series of independent MT insection events, which brought in the SatL repeats into the nuclear genome in the following order: SatL4B, SatL4A, SatL3/SatL2E, SatL2D/SatL2A, SatL2B/SatL2C, SatL1C, and SatL1B.

(B) Scatterplot for the repeat copy numbers for the nuclear SatL arrays (log10 scale on the *y*-axis) and SatL repeat consensus distance to the MT SatL1A repeats (*x*-axis). The fitted line using a linear regression model is shown in red. The SatL repeat copy number is significantly correlated with the evolutionary distance to SatL1A (Pearson's correlation coefficient $r = 0.969$, $P = 0.0003$ and Spearman's correlation coefficient $\rho = 0.964$, $P = 0.0028$).

(C) Scatterplot for the pairwise sequence identity within SatL arrays (*y*-axis) and SatL repeat consensus distance to the MT SatL1A repeats (*x*-axis). The fitted line using a linear regression model is shown in red. The SatL array pairwise identity is negatively correlated with the evolutionary distance to SatL1A (Pearson's correlation coefficient $r = -0.897$, $P = 0.0026$ and Spearman's correlation coefficient $\rho = -0.857$, $P = 0.0107$).

(D) Scatterplot for SatL repeat GC content (*y*-axis) and SatL repeat consensus distance to the MT SatL1A repeats (*x*-axis). The fitted line using a linear regression model is shown in red. A blue horizontal line is drawn at the *Nv* nuclear genome average GC content level. The SatL GC is negatively correlated with the evolutionary distance to SatL1A (Pearson's correlation coefficient $r = -0.972$, $P < 0.0001$ and Spearman's correlation coefficient $\rho = -0.905$, $P = 0.0046$).

(E) Scatterplot for MT/NuMT genic region GC content (*y*-axis) and SatL repeat consensus distance to the MT SatL1A repeats (*x*-axis). The fitted line using a linear regression model is shown in red. No significant correlation is observed ($P > 0.20$).

(F) The *Nv* SatL1A repeat region (***left***) is predicted to fold into a super-cruciform structure, with repeat number 1-2-3-4 paring with 29-28-27-26 (***right***). The darker blue arrows indicate the forward tandem repeats, while the light blue arrows are the inverted repeatR copies. This palindromic sequence paring allows frequent gene conversion events, resulting in GC-bias and repeat homogenization by compensatory substitutions. All three substitutions in the first and last four copies are compensatory, as shown in the upper-right corner.

(G) Barplot of SatL consensus sequence substitution numbers in the S-to-W (blue), W-to-S (purple), S-to-S (gray), and W-to-W (pink) categories, between neighboring SatL repeats during the evolutionary history (SatL3-L2, SatL2-1C, SatL1C-1B, and SatL1B-1A). S (strong): C or G. W (weak): A or T.

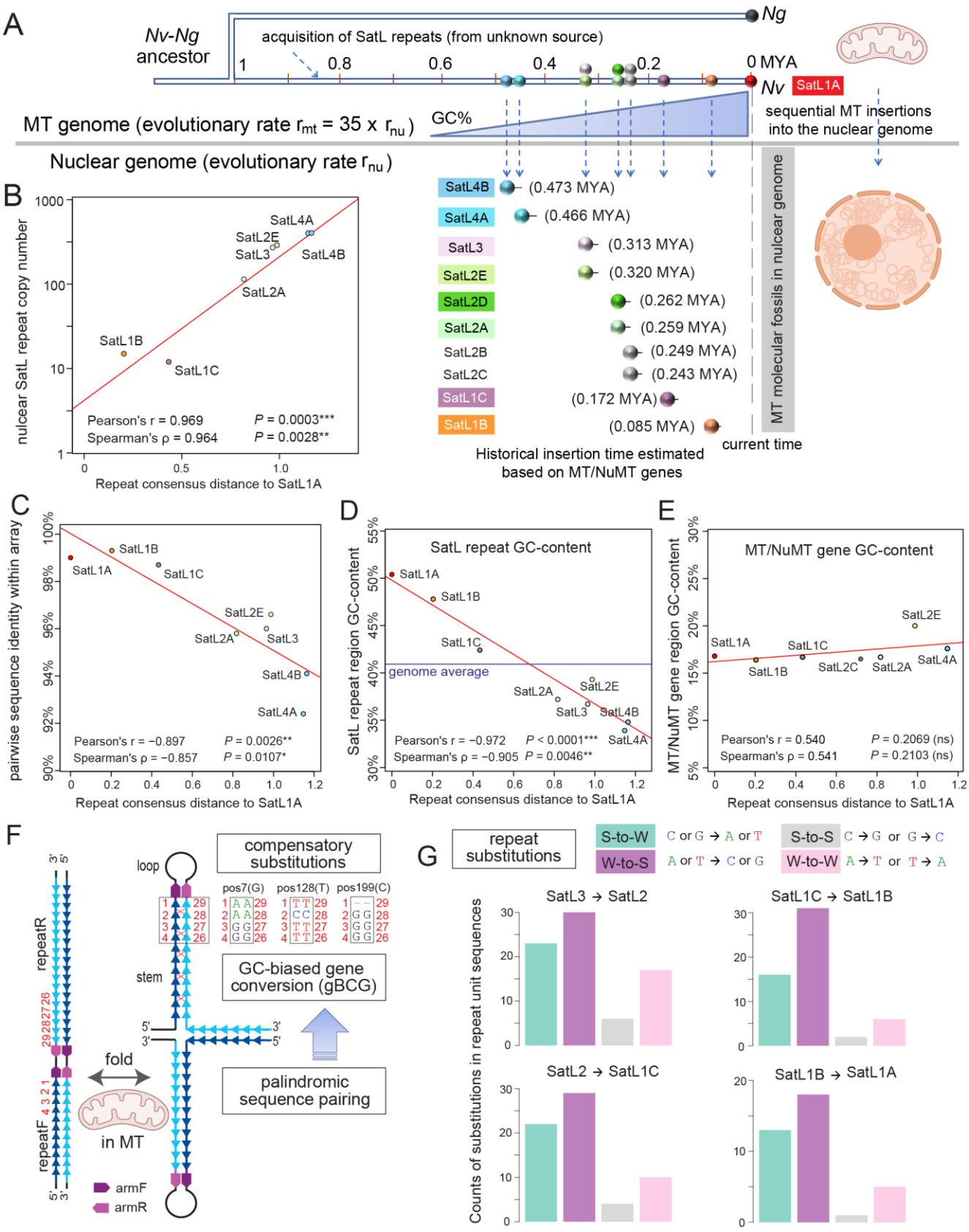
A
Nv-Ng ancestor
acquisition of SatL repeats (from unknown source)
Ng
Nv
SatL1A
0 MYA
MT genome (evolutionary rate r_{mt} = 35 x r_{nu})
GC%
sequential MT insertions into the nuclear genome
Nuclear genome (evolutionary rate r_{nu})
SatL4B (0.473 MYA)
SatL4A (0.466 MYA)
SatL3 (0.313 MYA)
SatL2E (0.320 MYA)
SatL2D (0.262 MYA)
SatL2A (0.259 MYA)
SatL2B (0.249 MYA)
SatL2C (0.243 MYA)
SatL1C (0.172 MYA)
SatL1B (0.085 MYA)
current time
MT molecular fossils in nulcear genome
Historical insertion time estimated based on MT/NuMT genes
B
nulcear SatL repeat copy number
Repeat consensus distance to SatL1A
Pearson's r = 0.969 P = 0.0003***
Spearman's ρ = 0.964 P = 0.0028**
C
pairwise sequence identity within array
Repeat consensus distance to SatL1A
Pearson's r = −0.897 P = 0.0026**
Spearman's ρ = −0.857 P = 0.0107*
D
SatL repeat region GC-content
genome average
Repeat consensus distance to SatL1A
Pearson's r = −0.972 P < 0.0001***
Spearman's ρ = −0.905 P = 0.0046**
E
MT/NuMT gene GC-content
MT/NuMT gene region GC-content
Repeat consensus distance to SatL1A
Pearson's r = 0.540 P = 0.2069 (ns)
Spearman's ρ = 0.541 P = 0.2103 (ns)
F
compensatory substitutions
pos7(G) pos128(T) pos199(C)
GC-biased gene conversion (gBCG)
palindromic sequence pairing
fold
in MT
loop
stem
repeatR
repeatF
armF
armR
G
repeat substitutions
S-to-W C or G → A or T
W-to-S A or T → C or G
S-to-S C → G or G → C
W-to-W A → T or T → A
SatL3 → SatL2
SatL1C → SatL1B
SatL2 → SatL1C
SatL1B → SatL1A
Counts of substitutions in repeat unit sequences

Fig. 4. Analyses of 403 repeat units in the SatL4B arrays identified the evolutionary history of four repeat unit types.

(A) Annotation of 403 repeat units in the SatL4B array. There are 17 copies of the ancestral 247bp units (dark blue), 218 copies of 216bp units (light blue), 109 copies of 137bp units (green), and 58 copies of 160bp units (orange). One novel singleton unit (143bp in length) was labeled in red (***bottom right***), 100 units were organized in 25 high-order 4-unit copies (216bp-160bp-137bp-216bp), which is labeled in gray boxes. 12 longer stretches of repetitive patterns were highlighted in color boxes, which consist of a total of 180 repeat units.

(B) Repeat unit evolution in the SatL4B array. The SatL4B ancestral 247bp-unit is color-coded in four consecutive sequence regions (I, II, III, and IV). The 112bp Region I has a GC content of 38.5% and is shared in all four repeat unit types. The 247bp-unit is 10bp shorted than the SatL4A unit, and they differ by six 1bp or 2bp deletion events. The 216bp-unit was derived from the 247bp-unit, with a 31bp deletion event in region III. The 137bp-unit consists of regions I and II, and the 160bp-unit contains regions I and IV.

(C) Boxplot of the number of nucleotide differences from SatL4A consensus in region I, for 137bp-units (green), 160bp-units (orange), 216bp-units (light blue), and 247bp-units (dark blue)

(D-E) Pairwise comparison of the number of nucleotide differences in region I for 401 SatL repeat copies, ordered by the physical location **(D)** and the four repeat unit categories **(E)**. The maximum number of differences (20) is presented in white and identical pairs were shown in red. A color gradient is used to demonstrate 0-20 differences.

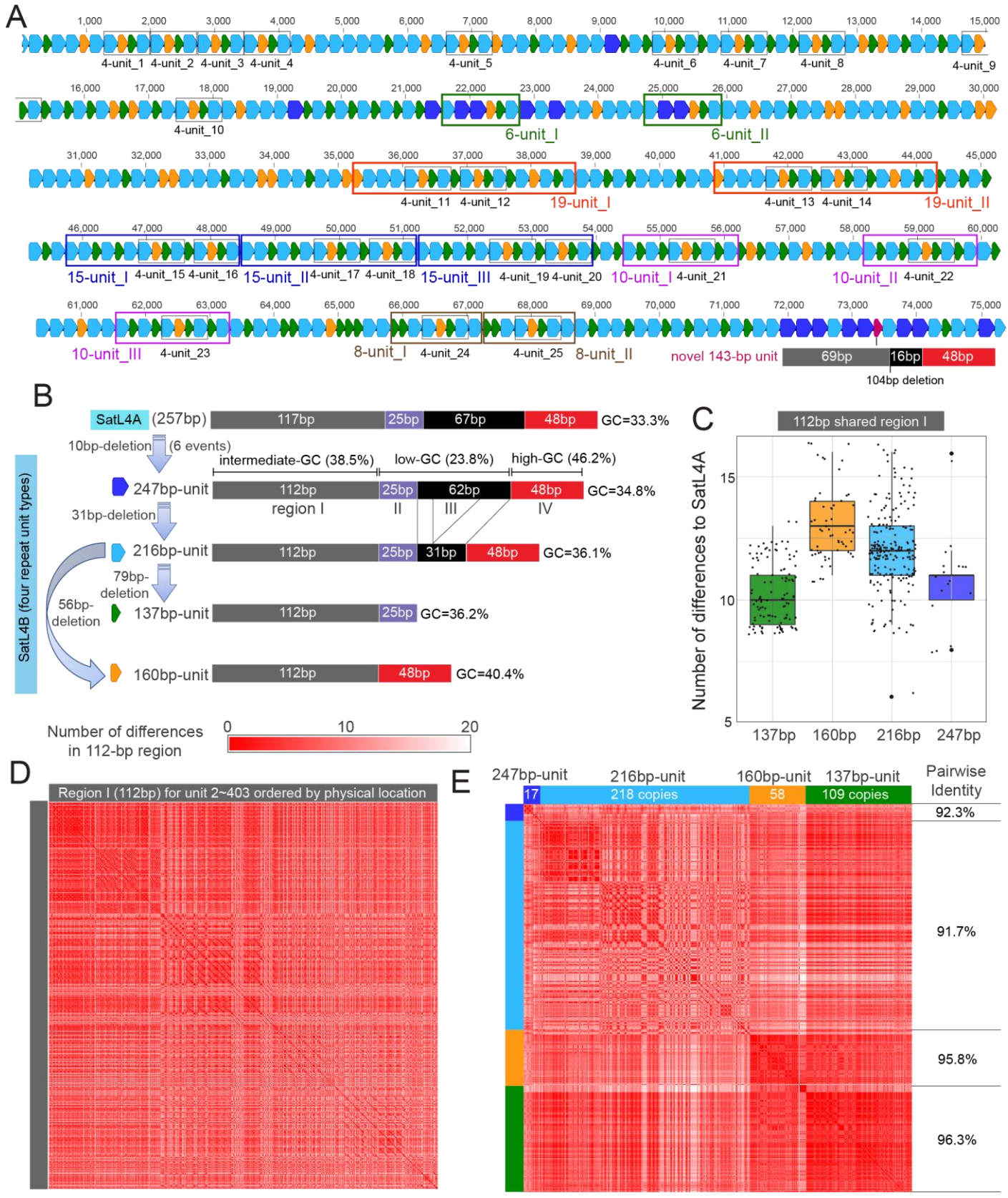
A
4-unit_1 4-unit_2 4-unit_3 4-unit_4
4-unit_5
4-unit_6 4-unit_7 4-unit_8
4-unit_9
4-unit_10
6-unit_I
6-unit_II
4-unit_11 4-unit_12
19-unit_I
4-unit_13 4-unit_14
19-unit_II
15-unit_I 4-unit_15 4-unit_16
15-unit_II 4-unit_17 4-unit_18
15-unit_III 4-unit_19 4-unit_20
10-unit_I 4-unit_21
10-unit_II 4-unit_22
10-unit_III 4-unit_23
8-unit_I 4-unit_24
4-unit_25 8-unit_II
novel 143-bp unit
69bp 16bp 48bp
104bp deletion
B
SatL4A (four repeat unit types)
SatL4A (257bp)
117bp 25bp 67bp 48bp GC=33.3%
10bp-deletion (6 events)
intermediate-GC (38.5%)
low-GC (23.8%)
high-GC (46.2%)
247bp-unit
112bp 25bp 62bp 48bp GC=34.8%
region I
II
III
IV
31bp-deletion
216bp-unit
112bp 25bp 31bp 48bp GC=36.1%
79bp-deletion
56bp-deletion
137bp-unit
112bp 25bp GC=36.2%
160bp-unit
112bp 48bp GC=40.4%
Number of differences in 112-bp region
0
10
20
C
112bp shared region I
Number of differences to SatL4A
15
10
5
137bp
160bp
216bp
247bp
D
Region I (112bp) for unit 2~403 ordered by physical location
E
247bp-unit
216bp-unit
160bp-unit
137bp-unit
17
218 copies
58
109 copies
Pairwise Identity
92.3%
91.7%
95.8%
96.3%

Fig. 5. Mitochondrial and nuclear SatL repeats discovered in *Muscidifurax raptorellus*, a closely-related parasitoid species to *Nv*.

(A) *Pteromalus puparum* (*Ppup*) and *Muscidifurax raptorellus* (*Mell*) are parasitoid wasp species in the same Pteromalinae subfamily, and they diverged from *Nasonia vitripennis* (*Nv*) 19 MYA and 4.9 MYA, respectively. The MT genome organization of these three species are plotted.

(B) The AT-rich *Ppup* MT control region repeats were found in four locations of its nuclear genome, with a total of 25 repeat units. 8 NuMT insertion events were discovered in the nuclear genome, and they are not in proximity with the MT repeat insertions.

(C) Genomic annotation of 12 NuMT regions in the *Mell* genome. A total of 90 repeat units were found in 5 NuMTs.

(D) Barplot of the GC content in nuclear and mitochondrial repeat arrays.